1978

NR-21

CONDENSATION HEAT TRANSFER OF STEAM FLOW ON ICE SURFACE

K. Trambauer
J. Straub

Technische Universität München
Lehrstuhl A für Thermodynamik

ABSTRACT

Under the aspects of nuclear reactor safety, experiments were conducted to determine the heat transfer rate of condensing steam flowing up- and downwards along a vertical ice surface. The test section was a 1 m long channel with a rectangular cross section of 140 x 70 mm^2, partially filled with ice. Temperatures, total pressure, static pressure of the steam, as well as the melting rate were measured. Furthermore, high speed pictures of the two phase flow were taken. The steam velocity was varied between 4 and 80 m/s at a pressure of approximately 1 bar. Melting rates of 0.6 to 6 mm/s were observed. No effect of the gravity on the liquid phase was detected at high steam velocity. With low velocities, the water film flowing downwards was not severely effected by the vapor counter flow. Both gravity and vapor-flow effects were equally efficient at moderate velocities. Therefore, a churn flow was observed as the steam flew upwards. The experimental data for the heat transfer coefficient were correlated to the vapor velocity by the equation $Nu = Nu_0 + C_2\ Re_v$.

NOMENCLATURE

c_p	specific heat capacity	J/kg K
g	acceleration of gravity	m/s^2
Δh	specific latent enthalpy	J/kg
$\dot{m}$	mass flux density	$kg/m^2\ s$
$\dot{q}$	heat flux density	W/m^2
$\dot{v}$	melting rate	$m^3/m^2\ s$
w	velocity	m/s
z	coordinate of hight	m
B	width of ice surface	m
D_h	hydraulic diameter	m
H	hight ice surface	m
$\dot{M}$	mass flow rate	kg/s
S	thickness of film	m
T	temperature	K
α	heat transfer coefficient	$W/m^2\ K$
η	dynamic viscosity	kg/ms
λ	thermal conductivity	W/mK
ν	kinematic viscosity	m^2/s
ρ	mass density	kg/m^3
τ_s	interfacial shear stress	N/m^2

Sub- and Superscripts

c	condensate
e	effective
i	ice
v	vapor
w	wall
-	averaged value

Dimensionless Numbers

$\beta = \tau_s / \rho\ (g\ \nu)^{2/3}$	interface friction
$C_q = (\dot{m}_{cv}\ \Delta h_v)/(\dot{m}_i\ \Delta h_i)$	enthalpy relation
$K_H = H(g/\ \nu^2)^{1/3}$	film number
$K_T = \lambda(T_v - T_w)/\eta \Delta h_e$	film number
$Nu = \alpha(\nu^2/g)^{1/3}\ /\lambda$	Nusselt number
$Pr = \eta\ c_p/\lambda$	Prandtl number
$Re = \dot{M}/B\eta$	Reynolds number
$Re_v = w_v D_h/\nu_v$	Reynolds number of vapor

INTRODUCTION

A blowdown results in a sudden pressure increase in the reactor containment. If the outflowing steam can be condensed the pressure increase will reduce and consequently reactor safety will be enhanced.

The "Ice Condensor" - a circular area, partially filled with ice, between the inner and outer part of the containment - is one possibility to reduce the pressure increase during blowdown. Tests with a subchannel of an ice condensor, which were conducted by Kraftwerk Union, Erlangen, showed the operation of this equipment. The research program which will be presented here was carried out to investigate the heat and mass transfer at the condensation of steam on a vertical ice surface. The steam velocity and flow direction as well as the flow cross section and testing time were varied to establish an empirical equation for the calculation of ice condensors and to compare the results with other experiments and theories.

PREVIOUS APPROACHES

If stagnant vapor condenses on a vertical, wet surface a condensate film is built up which flows downwards due to gravity. With the assumptions that the vapor is saturated, no noncondensable gas is present, the wall surface temperature is uniform, and the physical properties of the film are constant and uniform, the heat transfer coefficient of the laminar condensate film can be calculated by the equation of Nusselt (1)

$$\alpha = \left(\frac{g\ \rho^2\ \lambda^3\ \Delta h_v}{4\ \eta\ (T_v - T_w)\ z} \right)^{1/4} \qquad (1).$$

If steam condenses on an ice surface the mass flux of the film is increased by the molten ice. Eckhardt (2) pointed out that for small temperature differences between steam and ice the Nusselt equation is valid if the effective latent enthalpy is used instead of the specific latent enthalpy of vaporization

$$\Delta h_e = (\Delta h_i\ \Delta h_v)/(\Delta h_i + \Delta h_v) \qquad (2).$$

Using a simple energie balance one obtaines for the Reynolds number a function of the averaged Nusselt number

$$Re = \overline{Nu}\ K_H\ K_T \qquad (3)$$

and if the film is laminar for the local Nusselt number

$$Nu = 0.694\ Re^{-1/4}. \qquad (4).$$

The disagreement of this analytical solution with the experimental results is due to the ripples in the condensat layer, McAdams (3), and a non-linear temperature distribution in the laminar film, Rohsenow (4). Struve (5) recommended for the transition from laminar to turbulent film flow a constant Nusselt number Nu = 0.22 and for the turbulent film flow the equation

$$Nu = 0.014\ Re^{0.41} \qquad (5).$$

Similar relationships for higher film flow rates were suggested by Grigull (6), Colburn (7), and Wilke (8). Dukler (9) developed a numerical solution for laminar and turbulent film flow with and without interfacial shear stress to calculate the liquid film thickness and heat transfer coefficient as a function of the interfacial shear stress and the film flow rate.

Shekriladse (10) pointed out that the calculation of the interfacial shear stress by condensation of flowing vapor is similar to the wall shear stress of a gas flow with wall suction

$$\tau_s = \dot{m}_{cv}\ w_v \qquad (6).$$

Furthermore he calculated the heat transfer coefficient of the laminar film as a function of the vapor velocity. For the case of counter-current and co-current annular flow Hewitt and Wallis (11) et al. discussed briefly the topics of flooding and flow reserval. Empirical relationships to calculate the onset of flooding are given e.g. by Feind (12).

ESTIMATION OF THE HEAT TRANSFER COEFFICIENT

The heat transfer coefficient can be estimated if both heat flux density and temperature difference through the film are known. If the melting rate (13) is measured and ice subcooling neglected, the heat flux density through the ice surface can be calculated

$$\dot{q}_i = \dot{v}_i\ \rho_i\ \Delta h_i \qquad (7).$$

For a laminar film with linear temperature and parabolic velocity distribution the relation between the latent enthalpy flux density from steam to film and from film to ice surface is

$$C_q = \frac{1 + (5/8)c_p(T_v - T_w)/\Delta h_i}{1 + (3/8)c_p(T_v - T_w)/\Delta h_v} \qquad (8).$$

If for the definition of the heat transfer coefficient only the latent enthalpy of vaporization is used instead of the average enthalpy difference, the heat transfer coefficient is

$$\alpha = c_q \frac{\dot{V}_i \rho_i \Delta h_i}{T_v - T_w} \quad (9)$$

The local mass flux density of condensing vapor is

$$\dot{m}_{cv} = \alpha \frac{(T_v - T_w)}{\Delta h_v} \quad (10)$$

and the film mass flow at z = H

$$\dot{M} = \bar{\alpha} \frac{(T_v - T_w)}{\Delta h_e} B H \quad (11)$$

with the effective latent heat

$$\Delta h_e = \frac{c_q \Delta h_i \Delta h_v}{c_q \Delta h_i + \Delta h_v} \quad (12)$$

The wall temperature is approximately given by the ice melting temperature. The film property values are taken at the effective film temperature (14, 15)

$$T_e = T_w + C (T_v - T_w) \quad (13)$$

with the value of C = 0.30 and the vapor property values at the saturated temperature.

So it is possible by measuring the melting rate as well as velocity, pressure, and temperature of steam to calculate the Nusselt number as well as the Reynolds number for the condensate film and the steam flow.

TESTING FACILITY

The testing facility is shown in Fig. 1. To vary the flow direction the ice channel can be fitted in the up- and downward section of the testing facility.The steam mass flow rate is varied by different cross section of the orifice plates ($F = 6.5; 12.7; 23.7; 49.1; 93.9; 196\ mm^2$). The steam generator is an electric boiler with a power of 63 kW, a working pressure of 20 bar and a maximum continous steam mass flow rate of 0.022 kg/s. This mass flow rate is too small for the required vapor velocities. Therefore the steam generator works as a hot water reservoir with supplying steam during the testing time, Hardegen (16).

The ice channel has a length of 1000 mm and a cross section of $70 \times 140\ mm^2$. Both wide sides have windowpanes of thermo shock resistance glass. One narrow side is cooled to carry the ice block and has 5 mounting holes for the thermocouples, the other side carries 15 mounting holes for the temperature and pressure measuring probes. Between both 18 thermocouplechains are stretched to measure the melting rate. An intake channel with 500 mm length and similar cross section to the ice channel precedes the test section and ensures a steady reduction of cross section, dependent on the ice thickness. In the recondensor the rest of the steam is condensed by water spraying. The connecting pipes before the orifice plate have a diameter of 40 mm and after it one of 100 mm.

During the testing time temperature and melting rate of the ice were measured as well as the temperature, total and static pressure of the steam. Before and after each test the thickness of ice in the channel and the level of liquid in the steam generator were determined. The temperatures were measured by thermocouples, the pressure by pitot tubes with a transducer, and the melting rate by thermocouplechains. A thermocouplechain consists of an alternating series of constantan and nickel-chrome thermo wire pieces (each 10 mm long). This configuration results in a squarewave voltage signal during ice melting. With the computer controlled data aquisition system the measured values of 40 test points can be recorded with a maximum frequency of 6 kHz. Attempts were made to calculate the steam velocity from dynamic pressure values but the signals were disturbed by waterdrops in the vapor flow and condensation in the pressure probes. Therefore the vapor mass flux had to be calculated by using the pressure drop and the change of liquid level in the steam generator. Other measurements were not disturbed so that all necessary values for the estimation of the heat transfer coefficient were recorded.

RESULTS

Running experiments with a high vapor mass flow rate the steam supply was very discontinious since the pressure drop in the steam generator was irregular due to thermal nonequilibrium effects. At tests with low vapor mass flow the transient behaviour of the steam supply can be neglected. Generally the melting rate versus ice surface is rather nonuniform. One reason for this behaviour is the disturbance of the velocity distribution of the vapor flow through the too short intake. The other reason is the different flow pattern inside the ice channel.

The flow pattern of the climbing vapor flow at a free steam velocity of about 10 to

15 m/sec is rather interesting: In the lower part of the ice channel the film is carried upwards by the vapor flow, while in the upper part the film flows downwards. The flow becomes unstable and a oscillating annular flow is observed as well as an enhanced melting rate in this area.
If the vapor velocity is lower, the film flows downwards and only some drops are carried upwards. At higher vapor velocities, however, the whole film is carried upwards by the vapor flow. For this two cases the melting rate is similar to the melting rate at vapor flowing downwards with an equivalent velocity (Table 1 and 2).

The total pressure inside the ice channel is in the range of 0.95 to 1.15 bar and the vapor temperature is 98 to 104 °C if the noncondensable gas is blown out of the channel. Hence only wet or saturated steam is present. The measured ice temperature is in the range of -2 to -4 °C and is nearly constant during testing time. The subcooling enthalpy as well as temperature is neglected. The resulting error of the heat transfer coefficient of less than 1 %. Therefore the average temperature difference through the film can be approximated by $T_V - T_W = 100$ K.

The ratio of the latent enthalpy flux densities (Eqn. 8) is $C_q = 1.67$.

So it is possible to estimate the average heat transfer coefficient it the average melting rate is used (Eqn.9) as well as the average vapor velocity in the channel

$$\overline{w_V} = \frac{\overline{\dot{M}_V}}{\rho_V \, \overline{F}} \tag{14}$$

with the local and temporal average vapor mass flux $\dot{M}_V$ and flow cross section $\overline{F}$. This results, except the values of the unstable annular flow, are approximated with an accuracy of 20 % by the function

$$\frac{\overline{\alpha}}{\alpha_o} = C_1 + \frac{\overline{w_V}}{w_o} \tag{15}$$

for the range $1.5 < \overline{w_V} < 60$ m/s with the data $\alpha_o = 1$ kW/m²K; $C_1 = 3.5$; $w_o = 2.5$ m/s or in the corresponding dimensionless form

$$Nu = Nu_o + C_2 \, Re_V \tag{16}$$

for the range $6 \cdot 10^3 < Re_V < 3 \cdot 10^5$ with the data $Nu_o = 0.229$; $C_2 = 6.33 \cdot 10^{-6}$.

The values of the unstable annular flow at upwards flowing vapor are:

$\overline{\alpha} = 8$ to 12 kW/m²K; $\overline{w_V} = 8$ to 12 m/s

$Nu = 0.5$ to 0.8; $Re_V = 30\,000$ to 50 000.

Table 1: Experimental results for upward flowing vapor

No.	$\dot{M}_V$	$\dot{v}_i$	$\dot{M}_{cv}/\dot{M}_V$	w_V	$\overline{\alpha}$
-	g/s	mm/s	-	m/s	kW/m²K
002	228	4.12	0.29	54.3	21.0
003	230	4.26	0.29	53.7	21.7
006	238	4.13	0.27	55.9	21.1
007	218	5.00	0.36	45.7	25.5
013	140	2.60	0.29	33.1	13.3
016	146	2.78	0.3	31.7	14.2
017	155	2.51	0.26	35.0	12.8
019	148	2.58	0.28	33.0	13.2
021	90	1.94	0.34	18.4	9.9
023	96	1.98	0.33	20.3	10.1
024	90	1.92	0.34	18.9	9.8
025	95	2.03	0.34	19.4	10.4
026	49	1.75	0.56	8.1	8.9
027	51	2.01	0.62	8.0	10.3
028	54	1.79	0.52	10.5	9.1
029	52	2.17	0.66	9.0	11.1
031	29	1.03	0.39	7.0	5.3
032	30	1.08	0.51	6.3	5.5
034	30	1.08	0.4	5.1	5.5
036	30	1.03	0.49	6.6	5.3
037	16	0.86	0.26	4.2	4.4
039	16	0.93	0.28	2.8	4.7
040	16	0.97	0.48	2.4	4.9

Table 2: Experimental results for downward flowing vapor

No.	$\dot{M}_V$	$\dot{v}_i$	$\dot{M}_{cv}/\dot{M}_V$	w_V	$\overline{\alpha}$
-	g/s	mm/s	-	m/s	kW/m²K
170	237	5.22	0.35	42.7	26.6
169	282	5.94	0.33	56.1	30.3
168	283	5.37	0.3	57.8	27.4
167	285	4.34	0.24	66.9	22.1
164	152	3.31	0.34	32.6	16.9
163	148	3.26	0.35	31.5	16.6
162	161	3.38	0.33	36.5	17.2
161	151	3.26	0.34	27.2	16.6
159	105	1.96	0.3	19.9	10.0
158	105	2.20	0.33	23.5	11.2
157	103	2.07	0.32	21.6	10.6
156	100	2.09	0.33	20.6	10.7
154	56	1.51	0.43	11.9	7.7
153	56	1.55	0.44	11.8	7.9
152	57	1.46	0.41	8.8	7.4
151	57	1.49	0.41	8.7	7.6
150	31	1.05	0.54	4.5	5.4
149	31	1.09	0.56	6.7	5.6
148	31	1.09	0.56	6.7	5.6
147	31	1.06	0.54	6.8	5.4
145	16	0.88	0.78	1.9	4.5
143	16	0.91	0.63	3.3	4.6
141	14	0.76	0.86	1.6	3.9

DISCUSSION

The data obtained from the experiments and the approximated function are presented in dimensionless form in Fig. 2. For refer-reference, the predictions of Dukler for Pr = 5 which are of relevance to the present experiment are indicated in the same figure. The dimensionless interface friction ß was calculated by Equation (6) and the film Reynolds number by Equation (11). It can be seen that the present data for lower vapor velocities are smaller and for higher velocities are larger than the curve recommended by Dukler. He suggests that the whole condensate is in the film. It was observed, however, that a part of liquid was carried as drops by the high velocity vapor flow, so that the film thickness and heat resistance is smaller. This is confirmed by the value of the critical steam velocity for the onset of entrainment which is in the range of w_V = 5 to 17 m/s for the present experiments. If the vapor velocity is lower, the data are related with the heat transfer of falling water film without interface friction (Fig. 3). The present data for lower velocities are in the range of heat transfer coefficients which are recommended by Grigull, Colburn and Struve.

Furthermore it is remarkable that the approximated function (16) for $Re_V = 0$ yields nearly the same value for the Nusselt number for the transition range given by Struve.
The maximum film thickness, estimated through the graph given by Dukler, is in the range S = 0.75 to 1.20 mm. The Reynolds number of vapor Re_V = 42 500 which characterize the onset of flooding, results from the equation given by Feind (12)

$$Re_v = 88.8\ Re^{1/2}\left(\frac{\rho_v}{\rho}\right)^{2/5}\left(\frac{\eta}{\eta_v}\right)^{3/4}\left[0.039\left(\frac{D_h}{S}\right)^{5/4}-1\right] \quad (17)$$

It is seen that there is a very good agreement with the experimental data.

For the calculation of the relation of the latent enthalpy flux densities and the effective latent enthalpy a parabolic velocity and linear temperature distribution through the film was asumed. This hypothesis results in a essential error if the temperature distribution is non-linear.

CONCLUSION

A simple relationship has been presented which allows the determination of the heat transfer coefficient as a function of the vapor velocity as well as the range of instable annular flow of climbing vapor flow. Furthermore it has been shown that the known equations, which are valid for condensation without melting, can be applied to calculate the heat transfer at condensation on ice, if the effective latent enthalpy is used. It has been confirmed that the interfacial shear stress during condensation of flowing vapor does not differ from the shear stress on a dry permeable surface in an ambient flow of non condensing gas.

The influence of temperature difference, total pressure, Prandtl number and relation between hydraulic diameter and length of the condensator was not determined because these values were not varied.

ACKNOWLEDGEMENT

The authors wish to acknowledge the financial support of the Bundesministerium für Forschung und Technologie of Federal Republic of Germany.

REFERENCES

1. Nusselt, W., Zeitschr. VDI, Vol.60, p. 541- 546, p. 569-575, 1910
2. Eckhardt, H., Wärmeübertragung von kondensierendem Dampf an schmelzende Wände, Thesis, TH Darmstadt, 1966
3. McAdams, W.H., Heat Transmission, 3 rd Edition, McGraw Hill, 1954
4. Rohsenow, W.M., Trans. ASME, Vol. 78, p. 1645-1648, 1956
5. Struve, H., VDI-Forsch.Heft 534, 1970
6. Grigull, U., Forsch.Geb.Ing.Wes., Vol. 18, p. 10-12, 1952
7. Colburn, A.P., Ind.Eng.Chem., Vol. 26, p. 432-434, 1934
8. Wilke, W., VDI-Forsch.Heft 490, 1962
9. Dukler, A.E., Chem.Eng.Prog.Symp. Series, No.30,Vol.56,p.1-10, 1960
10. Shekriladze, I.G., Heat Trans.Sov.Res., Vol. 4, p. 99-112, 1972
11. Hewitt, G.F. and Wallis, G.B., Flooding and associated phenomena in falling flow in a tube, AERE-R 4022
12. Feind, K., VDI-Forsch.Heft 481, 1960
13. Turcotte, P., Jour.Fluid Mech. Vol.8, p. 123-129, 1960
14. Minkowycz, W.J. and Sparrow, E.M., Int. JHMT, Vol. 9, p.1125-1144, 1966
15. Drew, T.B. and Mueller, A.C., Trans. AICE, Vol. 33, p. 449-471, 1937
16. Hardegen, H., Zur Berechnung der Arbeitsweise von Heißwasserspeichern, Thesis, TU Braunschweig, 1972.

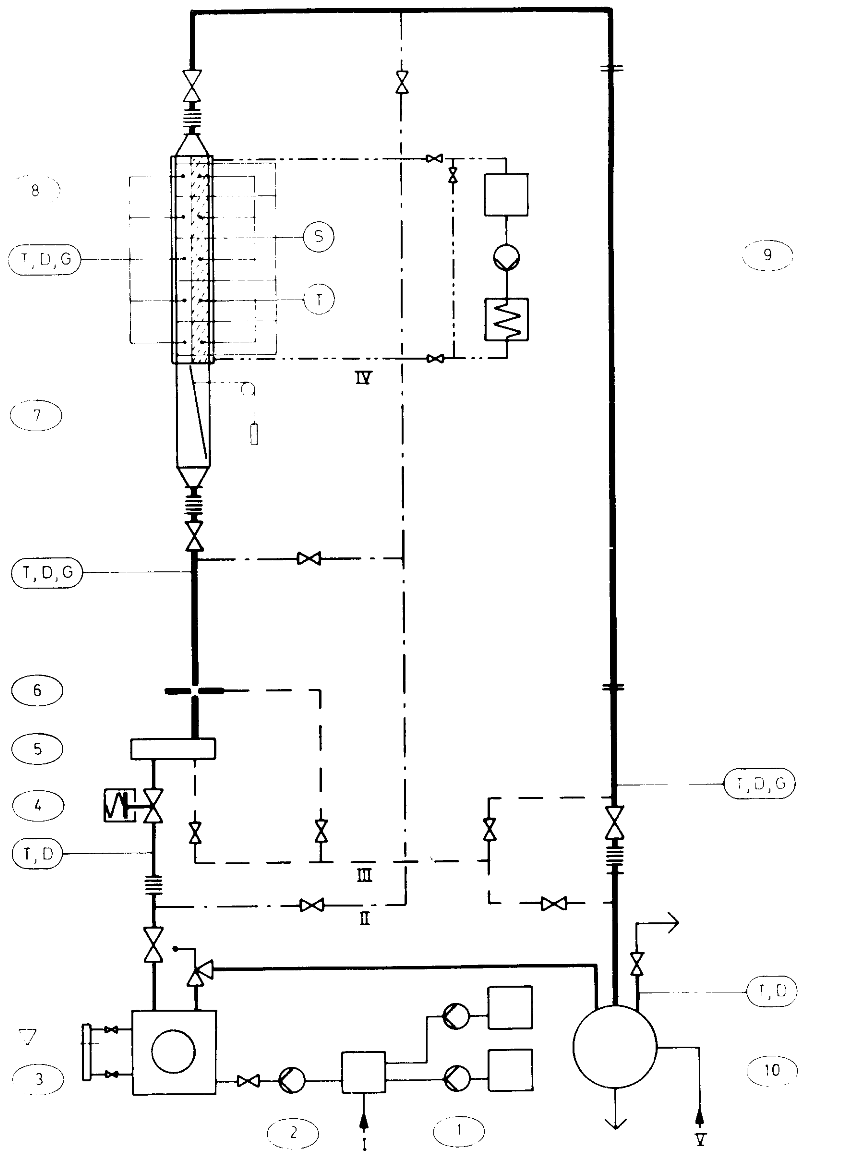

Measured variable	1 Dosing station	6 Orifice plate	I Feed water
T Temperature	2 Feed water pump	7 Intake channel	II Steam heating
D Pressure	3 Steam genetator	8 Ice channel	III Steam trap
G Velocity	4 Main valve	9 Coolant pump	IV Coolant line
S Melting rate	5 Drop catcher	10 Recondensor	V Cooling water

Fig. 1: Schematic diagramm of test facility

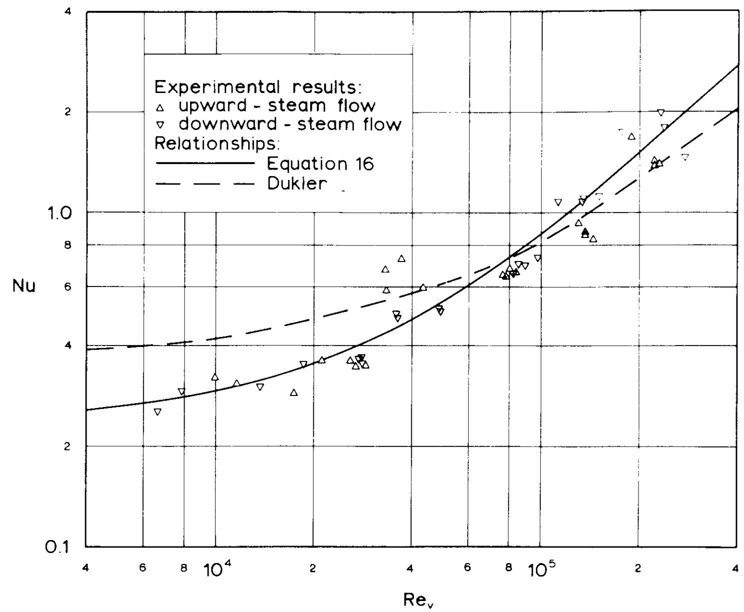

Fig. 2: Nusselt number vs Reynolds number of vapor

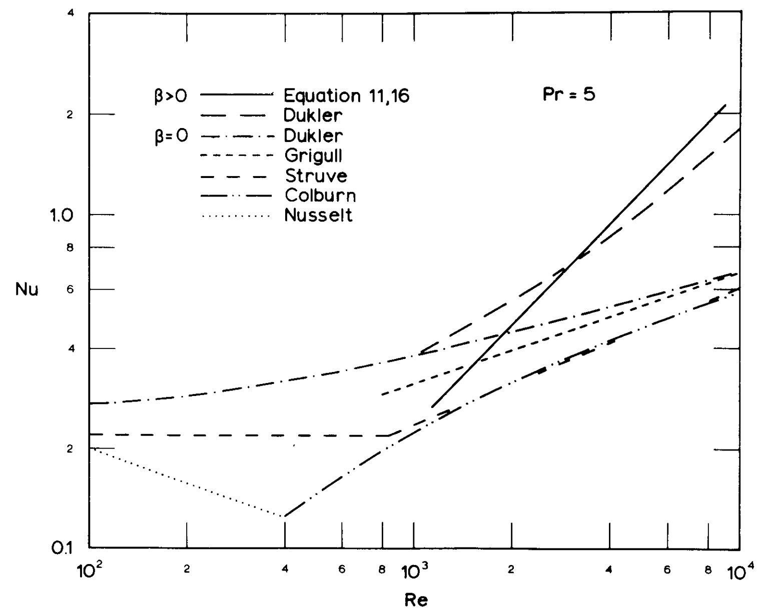

Fig. 3: Nusselt number vs Reynolds number of film.